Exact Sampling Results for Some Classes of Parametric Nonbandlimited 2-D Signals

Irena Maravić and Martin Vetterli, *Fellow, IEEE*

***Abstract*—We present sampling results for certain classes of two-dimensional (2-D) signals that are not bandlimited but have a parametric representation with a finite number of degrees of freedom. While there are many such parametric signals, it is often difficult to propose practical sampling schemes; therefore, we will concentrate on those classes for which we are able to give exact sampling algorithms and reconstruction formulas. We analyze in detail a set of 2-D Diracs and extend the results to more complex objects such as lines and polygons. Unlike most multidimensional sampling schemes, the methods we propose perfectly reconstruct such signals from a finite number of samples in the noiseless case. Some of the techniques we use are already encountered in the context of harmonic retrieval and error correction coding. In particular, singular value decomposition (SVD)-based methods and the annihilating filter approach are both explored as inherent parts of the developed algorithms. Potentials and limitations of the algorithms in the noisy case are also pointed out. Applications of our results can be found in astronomical signal processing, image processing, and in some classes of identification problems.**

***Index Terms*—Annihilating filters, critical sampling, Fourier series, signals of finite complexity, singular value decomposition.**

I. Introduction

SAMPLING theory has been a topic of extensive research over the past few decades, which led to refinements of the foundations of Shannon's theory and the development of more general formulations with immediate relevance to signal processing and communications. For example, it is already well known that the traditional sampling theorem for representation of bandlimited functions can be extended to classes of nonbandlimited signals that belong to shift-invariant spaces, such as uniform splines [1], [16]. While this result is valid for signals that live on a subspace spanned by a generating function and its uniform shifts, it cannot be extended to a general case, and typically, only the projection of the signal onto that specific subspace can be reconstructed.

Recently, it was shown that it is possible to develop sampling schemes for a larger class of signals that are neither bandlimited nor live on a subspace, namely, certain signals of a finite innovation rate [20]. Examples of such signals include streams of Diracs, nonuniform splines, and piecewise polynomials, with the common feature that they allow for a parametric representation with a finite number of degrees of freedom and can be perfectly reconstructed from a finite set of samples. The proposed methods were intended for one-dimensional (1-D) signals, but when going to higher dimensions, the problem becomes more involved and does not allow direct extension of 1-D results. In this paper, we consider the problem of developing exact sampling schemes and reconstruction formulas for certain classes of parametric nonbandlimited 2-D signals that have a finite number of degrees of freedom. The sampling setup we will be using is shown in Fig. 1, where the original 2-D signal $g(x,y)$ is filtered with a smoothing kernel $\varphi(x,y)$, and a uniform set of samples is taken from the filtered version $g_f(x,y) = g(x,y) * \varphi(x,y)$, that is

$$g_s(p,q) = \langle g(x,y), \varphi(x - pT_{sx}, y - qT_{sy}) \rangle \ , \ p,q \in \mathbb{Z}. \quad (1)$$

The above setup is typical for acquisition devices encountered in practice, and the key question is under what conditions we can reconstruct $g(x,y)$ from $g_s(p,q)$. While this question is fundamental in signal processing, the problem we consider differs from standard problems in sampling theory in the following way. Namely, the space of signals we analyze is not a vector space but, rather, a nonlinear space of finite dimension, whereas the classic assumption is that the signals belong to shift-invariant vector spaces (e.g. bandlimited space or spline spaces [16]).

There are a few important issues that will be addressed throughout the paper. We investigate if it is possible to develop a sampling scheme for a signal with M degrees of freedom that requires on the order of M samples and which kernels $\varphi(x,y)$ allow for such a scheme. In effect, this would substantially reduce computational and storage requirements compared to existing methods. Another important point is the numerical performance of the algorithms, i.e., we will be interested in developing techniques that can recover the signal from a set of its samples with high numerical precision, regardless of the signal

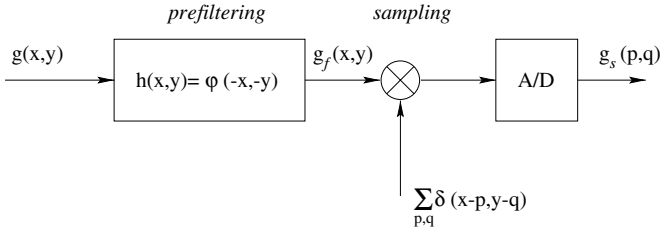

Fig. 1. Sampling setup analog signal $g(x,y)$ is prefiltered with $h(x,y) = \varphi(-x,-y)$ (anti-aliasing step). The sampled signal is given by $g_s(p,q) = \sum_{p,q \in \mathbb{Z}} g_f(x,y)\delta(x-p, y-q)$.

Manuscript received February 21, 2002; revised March 7, 2003. The associate editor coordinating the review of this paper and approving it for publication was Dr. Olivier Cappe.

I. Maravić is with the IC, Swiss Federal Institute of Technology, CH-1015 Lausanne, Switzerland (e-mail: Irena.Maravic@epfl.ch).

M. Vetterli is with the IC, Swiss Federal Institute of Technology, Lausanne, Switzerland, and with the Electrical Engineering and Computer Science Department, University of California at Berkeley, Berkeley CA 94720 USA (e-mail: Martin.Vetterli@epfl.ch).

Digital Object Identifier 10.1109/TSP.2003.819984

complexity (e.g., the value of the parameter M) or signal structure. Finally, we expect the algorithms to be computationally efficient and, if possible, robust to noise and model mismatch. We will show that under certain conditions, one can develop methods that satisfy all of the above requirements. Some of the techniques we will be using are encountered in spectral analysis [6]–[12], [14], [15], [17]–[19] or in error correction coding [2], [3], [10]. The proposed methods, while being more complex than the existing schemes for bandlimited signals, still offer efficient algorithmic implementations. We will analyze in detail the case of a signal made up of 2-D Diracs, which is of particular interest to the field of astronomical image processing, and discuss a possible extension of the results to the problem of sampling some simple objects, such as lines and polygons.

The outline of the paper is as follows. In Section II, we review classes of nonbandlimited two-dimensional (2-D) signals that will be of interest in the sequel. In Section III, we develop sampling methods for a periodic set of M Diracs in two dimensions in continuous space and extend the results to signals that can be modeled as a convolution of Diracs and a known point spread function. In Section IV, we consider the problem of sampling finite length signals and derive sampling theorems using the Gaussian kernel. A possible application of the previous results to the problem of sampling some simple objects, such as polygons, is addressed in Section V. In Section VI, we analyze the problem of estimating the model order and discuss numerical performance of the proposed methods as well as their robustness to model mismatch and noise. In particular, we modify the algorithms in order to improve their numerical precision in the case of noisy data. Simulation results that indicate desirable properties both in the deterministic case and in the presence of noise are given in Section VII. We also address limitations due to ill-conditioning in the Gaussian finite length case. Finally, we discuss some directions for future work in the concluding remarks.

II. Two-Dimensional Signals of Finite Complexity

An intuitive way to introduce the concept of signals of finite complexity is to think of them as having a parametric representation with a finite number of degrees of freedom. The main reason for considering the sampling problem for such a class of signals is the fact that the number of degrees of freedom can be often directly related to the minimum sampling density ρ or to the minimum number of samples that allows for a perfect reconstruction. For example, consider the simple case of a 2-D bandlimited real signal $g(x,y)$, with a Fourier transform that is nonzero over a finite region R in the frequency space. If we let $2B_x$ and $2B_y$ represent the widths in the f_x and f_y directions of the smallest rectangle that encloses the region R, then appropriately spaced samples can perfectly represent the signal, i.e.,

$$g(x,y)=\sum_{m=-\infty}^{\infty}\sum_{n=-\infty}^{\infty} g(mX,nY)\operatorname{sinc}\left(\frac{x}{X}-m,\frac{y}{Y}-n\right) \tag{2}$$

where X and Y are such that $X\le 1/(2B_x)$ and $Y\le 1/(2B_y)$. The above relation implies that we can think of the bandlimited signal as having $1/X$ and $1/Y$ degrees of freedom per unit of length in the x and y direction, respectively, which correspond to minimum sampling densities ρ_x and ρ_y. A more general form of (2) is given by

$$g(x,y)=\sum_{m=-\infty}^{\infty}\sum_{n=-\infty}^{\infty} c_{mn}\varphi\left(\frac{x-x_m}{X},\frac{y-y_n}{Y}\right) \tag{3}$$

where x_m and y_n are arbitrary shifts. For example, when $\varphi(x,y)=\delta(x,y)$ and both x_n-x_{n-1} and y_n-y_{n-1} are i.i.d. random variables with exponential density, then $g(x,y)$ describes a separable 2-D Poisson process. Other examples of finite complexity signals include simple lines and polygonal lines, planar parametric curves, as well as some parametric signals whose boundaries have a finite number of degrees of freedom. In general, the space of signals we will be considering is a finite-dimensional nonlinear space. By exploiting this property, we will develop sampling schemes that allow for a perfect reconstruction from a finite number of samples.

III. Periodic Set of 2-D Diracs in Continuous Space

A. Fourier Series

One of the most basic forms of nonbandlimited signals of finite complexity is a set of Diracs, that is, one particular realization of a 2-D Poisson process. Although this signal has a simple parametric representation, the problem of extracting its parameters from a set of samples is a more involved task than in the 1-D case. In this section, we present sampling methods for a periodic set of Diracs in continuous space. Specifically, we will show that a lowpass approximation of the signal, which is essentially a projection of the signal onto the subspace of proper dimension, provides sufficient information for perfect reconstruction.

Let $g(x,y)$ be a periodic 2-D signal given by

$$g(x,y)=\sum_{p,q}\sum_{k=0}^{M-1} c_k\delta(x-pT_x-x_k,y-qT_y-y_k) \tag{4}$$

where M is assumed to be known, and $T_x=T_y=T$. Consider the Fourier series representation of $g(x,y)$

$$g(x,y)=\sum_{m=-\infty}^{\infty}\sum_{n=-\infty}^{\infty} G[m,n]e^{jm\omega_0 x}e^{jn\omega_0 y} \tag{5}$$

where $\omega_0=(2\pi/T)$ and $G[m,n]$ are the Fourier series coefficients given by

$$G[m,n]=\frac{1}{T^2}\int_0^T\int_0^T g(x,y)e^{-jm\omega_0 x}e^{-jn\omega_0 y}dxdy \tag{6}$$

$$=\frac{1}{T^2}\int_0^T\int_0^T\sum_{k=0}^{M-1} c_k\delta(x-x_k,y-y_k)\times e^{-jm\omega_0 x}e^{-jn\omega_0 y}dxdy \tag{7}$$

$$=\sum_{k=0}^{M-1}\frac{1}{T^2}\int_0^T\int_0^T c_k\delta(x-x_k,y-y_k)\times e^{-jm\omega_0 x}e^{-jn\omega_0 y}dxdy \tag{8}$$

$$= \sum_{k=0}^{M-1} \frac{1}{T^2} c_k e^{-jm\omega_0 x_k} e^{-jn\omega_0 y_k}$$
$$= \sum_{k=0}^{M-1} a_k e^{-jm\omega_0 x_k} e^{-jn\omega_0 y_k} \quad (9)$$

that is, a linear combination of M complex exponentials. We will first analyze the case where the set of Diracs has no common components along one direction, that is, all x_k are distinct (or alternatively all y_k have different values) and present a method that can perfectly recover the signal from $\mathcal{O}(M)$ samples.

B. Annihilating Filter Method for the Separable Case

Consider the Fourier Series coefficients $G[m,0]$ and $G[m,1]$ given by (9)

$$G[m,0] = \sum_{k=0}^{M-1} a_k e^{-jm\omega_0 x_k} \quad (10)$$
$$G[m,1] = \sum_{k=0}^{M-1} a_k e^{-jm\omega_0 x_k} e^{-j\omega_0 y_k} = \sum_{k=0}^{M-1} A_k e^{-jm\omega_0 x_k} \quad (11)$$

where $A_k = a_k e^{-j\omega_0 y_k}$, and define a filter $H(z)$ of order M, having zeros at $z_k = e^{-j\omega_0 x_k}$

$$H(z) = \prod_{k=0}^{M-1} (1 - z^{-1} z_k) = \sum_{i=0}^{M} h_i z^{-i}. \quad (12)$$

Let $H = \text{coeff}(H(z)) = [1\ h_1\ h_2 \ldots h_M]$. Since $G[m,1]$ has the form of a weighted sum of exponentials, i.e., $G[m,1] = \sum_{k=0}^{M-1} \alpha_k z_k^m$, the following relation must be satisfied:

$$H * G[m,1] = 0, \quad m \in \mathbb{Z}. \quad (13)$$

In other words, each exponential in $G[m,1]$ is being zeroed out by one of the roots of $H(z)$; thus, the filter $H(z)$ is called the annihilating filter, and its zeros uniquely define the set of locations $\{x_k\}$. A more detailed analysis of the annihilating filters is given in [15] and [20]. Therefore, we will only outline the basic steps of the algorithm and discuss its application to the 2-D problem.

Annihilating Filter Algorithm:

- Find the Fourier series coefficients $G[m,0]$ and $G[m,1]$, $m \in [-M, M]$ from a set of samples

$$y_s[p,q] = \langle g(x,y), \varphi(x - pT_{sx}, y - qT_{sy}) \rangle$$
$$p \in \left[0, \frac{T}{T_{sx}} - 1\right], \quad q \in \left[0, \frac{T}{T_{sy}} - 1\right] \quad (14)$$

where $\varphi(x,y)$ is a 2-D sinc sampling kernel[1] of bandwidth $[-M\omega_0, M\omega_0] \times [-\omega_0, \omega_0]$, whereas the sampling periods T_{sx} and T_{sy} are chosen such that $N_{sx} = T/T_{sx} \geq 2M+1$ and $N_{sy} = T/T_{sy} \geq 2 \cdot 1 + 1$, with $\{N_{sx}, N_{sy}\} \in \mathbb{N}$. Namely, the sample values $y_s[p,q]$ are given by

$$y_s[p,q] = \sum_m \sum_n G[m,n] \times \left\langle \varphi(x - pT_{sx}, y - qT_{sy}), e^{jm\omega_0 x} e^{jn\omega_0 y} \right\rangle \quad (15)$$
$$= \sum_m \sum_n G[m,n] \Phi(m\omega_0, n\omega_0) \times e^{jm\omega_0 pT_{sx}} e^{jn\omega_0 qT_{sy}} \quad (16)$$
$$= \sum_{m=-M}^{M} \sum_{n=-1}^{1} G[m,n] e^{jm\omega_0 pT_{sx}} e^{jn\omega_0 qT_{sy}} \quad (17)$$

where $\Phi(\omega_x, \omega_y)$ is the Fourier transform of $\varphi(x,y)$, which satisfies

$$\Phi(\omega_x, \omega_y) = \begin{cases} 1, & |\omega_x| \leq M\omega_0,\ |\omega_y| \leq \omega_0 \\ 0, & \text{otherwise.} \end{cases} \quad (18)$$

If the sampling periods T_{sx} and T_{sy} satisfy the above requirements, this system of equations is invertible and will yield a unique solution for $G[m,0]$ and $G[m,1]$, $m \in [-M, M]$.

- Find the filter coefficients h_i, $i = 1, 2, \ldots, M$ from a system of equations

$$H * G[m,1] = \sum_{i=0}^{M} h_i G[m-i,1] = 0. \quad (19)$$

If we let $m = 1, 2, \ldots, M$, the above system reduces to

$$h_0 G[m,1] + \sum_{i=1}^{M} h_i G[m-i,1] = 0. \quad (20)$$

Assuming without loss of generality that $h_0 = 1$, the filter coefficients h_i can be computed from the Yule–Walker system

$$\sum_{i=1}^{M} h_i G[m-i,1] = -G[m,1], \quad m = 1, 2, \ldots, M \quad (21)$$

which has a unique solution if the x_k's are distinct. If that condition is satisfied, the Fourier series coefficients $G[m,1], m \in [-M+1, M]$ provide sufficient information to solve uniquely for the filter coefficients h_i and, hence, for the set $\{x_i\}$ by factorization.

- Solve for the set of pairs (x_k, y_k) and corresponding weights a_k.

Consider the expressions for $G[m,0]$ and $G[m,1]$, $m \in [0, M-1]$ in a matrix form

$$\begin{pmatrix} G[0,0] \\ G[1,0] \\ \vdots \\ G[M-1,0] \end{pmatrix} = \begin{pmatrix} 1 & \cdots & 1 \\ e^{-j\omega_0 x_0} & \cdots & e^{-j\omega_0 x_{M-1}} \\ \vdots & \ddots & \vdots \\ e^{-j(M-1)\omega_0 x_0} & \cdots & e^{-j(M-1)\omega_0 x_{M-1}} \end{pmatrix} \times \begin{pmatrix} a_0 \\ a_1 \\ \vdots \\ a_{M-1} \end{pmatrix}. \quad (22)$$

[1]Note that $\varphi(x,y)$ does not necessarily have to be a periodic function.

The above system is a Vandermonde system that yields a unique solution for the weights a_i, provided $x_i \neq x_j$ when $i \neq j$. By a similar argument, $A_i = a_i e^{-j\omega_0 y_i}$ can be found from the coefficients $G[m,1]$

$$\begin{pmatrix} G[0,1] \\ G[1,1] \\ \vdots \\ G[M-1,1] \end{pmatrix} = \begin{pmatrix} 1 & \dots & 1 \\ e^{-j\omega_0 x_0} & \dots & e^{-j\omega_0 x_{M-1}} \\ \vdots & \ddots & \vdots \\ e^{-j(M-1)\omega_0 x_0} & \dots & e^{-j(M-1)\omega_0 x_{M-1}} \end{pmatrix} \times \begin{pmatrix} a_0 e^{-j\omega_0 y_0} \\ a_1 e^{-j\omega_0 y_1} \\ \vdots \\ a_{M-1} e^{-j\omega_0 y_{M-1}} \end{pmatrix}. \quad (23)$$

Equations (21)–(23) yield a unique solution for the set $\{(x_k, y_k, a_k)\}$; thus, we can state the following proposition.

Proposition 1: Let $g(x,y)$ be a periodic set of M weighted 2-D Diracs of periods $T_x = T_y = T$ in the x and y directions, and assume that $g(x,y)$ does not contain common components along the x direction. Denote by $\varphi(x,y)$ the 2-D sinc sampling kernel of bandwidth $[-M\omega_0, M\omega_0] \times [-\omega_0, \omega_0]$, and choose the sampling periods T_{sx} and T_{sy} such that $N_{sx} = T/T_{sx} \geq 2M+1$ and $N_{sy} = T/T_{sy} \geq 2 \cdot 1 + 1$, where $\{N_{sx}, N_{sy}\} \in \mathbb{N}$. Then, the samples

$$y_s[p,q] = \langle g(x,y), \varphi(x - pT_{sx}, y - qT_{sy}) \rangle \qquad p \in [0, N_{sx}-1], \quad q \in [0, N_{sy}-1]$$

are a sufficient representation of $g(x,y)$.

In the case when the coordinates of the Diracs are distinct along the y direction but not along the x direction, the algorithm remains virtually the same. The only difference is the use of an alternative sinc sampling kernel of bandwidth $[-\omega_0, \omega_0] \times [-M\omega_0, M\omega_0]$, whereas the signal parameters can be found from the Fourier series coefficients $G[0,n]$ and $G[1,n]$, $n \in [-M, M]$. The presented method thus yields a unique solution by taking only $\mathcal{O}(M)$ samples of the signal, but its numerical stability typically degrades as the number of Diracs increases due to the root-finding part of the algorithm. Another disadvantage is that the method fails when the Diracs have common components along both directions, which also points to numerical instability if the coordinates are very close.

It is worth noting that it is also possible to solve for the signal parameters from the same set of the Fourier series coefficients by using alternative algorithms, based on 1-D subspace methods for harmonic retrieval, such as ESPRIT [8] or the state space method [12]. As opposed to the annihilating filter algorithm, a basic principle inherent in the subspace methods is the singular value decomposition (SVD). However, the same necessary condition for the success of these methods holds, namely, the set of Diracs must have no common components along the x or the y direction. If such is not the case, one possible way of handling this problem is discussed in the next subsection.

C. Sampling Schemes in the Nonseparable Case

The algorithm we described is based on the idea of reducing the 2-D sampling problem to one dimension and applying the 1-D annihilating filter method. We have seen that this approach imposes certain constraints in terms of the locations of the Diracs in the set, i.e., the necessary condition is that the problem is separable in the x, or alternatively, y direction. In order to avoid this constraint, it seems natural to try to extend the idea of annihilating filters to two dimensions. In other words, if we can find an FIR filter $H(z_1, z_2)$ having M zeros at $(z_{1k}, z_{2k}) = (e^{-j\omega_0 x_k}, e^{-j\omega_0 y_k})$, which satisfies $H[m,n] * G[m,n] = 0$, then the problem would essentially be equivalent to the one we discussed in the 1-D case. Yet, it turns out that this approach cannot be used. The main reason is that in the 2-D case, there is no general relationship between the degree of a bivariate polynomial and the number of its zeros. For example, consider a filter $H(z_1, z_2) = \prod_{k=0}^{M} (1 - z_1^{-1} e^{-j\omega_0 x_k} z_2^{-1} e^{-j\omega_0 y_k})$ that is a 2-D counterpart of the annihilating filter defined in Section III. $H(z_1, z_2)$ is a polynomial in z_1^{-1} and z_2^{-1} of degree $2M$ and satisfies the relation $H[m,n] * G[m,n] = 0$ but has an infinite number of zeros over the complex field, which is located at hyperbolas $z_1 z_2 = e^{-j\omega_0(x_k + y_k)}$. Clearly, the problem in two dimensions is more involved, and a simple extension of the method from the 1-D case will not lead to the solution.

An alternative way to estimate the locations and weights of Diracs is to use the SVD as the inherent part of the algorithm. Two-dimensional SVD-based algorithms have been studied extensively in the context of harmonic retrieval, typically for distinguishing and tracking signals of interest and extracting relevant information from noisy measurements. In that particular framework, subspace methods are used with the aim to estimate the signal parameters from noisy data, and a model that approximately fits all the available information is more desirable. We will prove that in the deterministic case, 2-D subspace methods can be adapted in such a way that the exact values of the parameters x_i, y_i, and a_i can be found from only $\mathcal{O}(M^2)$ samples of the signal $g(x,y)$.

D. Subspace Methods

Consider again the Fourier series coefficients $G[m,n]$ given by (9)

$$G[m,n] = \sum_{k=0}^{M-1} a_k e^{-jm\omega_0 x_k} e^{-jn\omega_0 y_k}. \quad (24)$$

To make the notation simpler, we can write the above system as

$$G[m,n] = \sum_{k=0}^{M-1} a_k w_k^m z_k^n \quad (25)$$

where $w_k = e^{-j\omega_0 x_k}$, and $z_k = e^{-j\omega_0 y_k}$. If we let $0 < m \leq P-1$ and $0 < n \leq Q-1$, (25) can be written as $G = WAZ$, with matrices W, A, and Z defined as

$$W = \begin{pmatrix} 1 & 1 & 1 & \dots & 1 \\ w_1 & w_2 & w_3 & \dots & w_M \\ \vdots & & & & \\ w_1^{P-1} & w_2^{P-1} & w_3^{P-1} & \dots & w_M^{P-1} \end{pmatrix} \quad (26)$$

$$A = \operatorname{diag}(a_1 \quad a_2 \quad a_3 \quad \dots \quad a_M) \quad (27)$$

$$Z = \begin{pmatrix} 1 & z_1 & z_1^2 & \dots & z_1^{Q-1} \\ 1 & z_2 & z_2^2 & \dots & z_2^{Q-1} \\ \vdots & & & & \\ 1 & z_M & z_M^2 & \dots & z_M^{Q-1} \end{pmatrix}. \tag{28}$$

If projections of the set of Diracs on the x and the y directions are distinct, then the rank of the matrix G is equal to M, and the values w_i and z_i can be obtained from the principal left or right singular vectors of G. If this condition is not satisfied, the algorithm fails due to the rank deficiency of G. Among the earliest spectral estimation techniques that addressed this problem was the matrix enhancement and matrix pencil (MEMP) algorithm [7]. The method introduces so-called "enhanced matrices," both of rank M, from which the sets $\{w_i\}$ and $\{z_i\}$ could be obtained, yet an additional step is required to form the correct pairs (w_i, z_i). This often involves a costly minimization procedure, making this algorithm unattractive due to its computational cost. In response to that, there has been a lot of work toward developing high-resolution methods that would link the estimation problems in both dimensions [6], [14], [17]–[19]. We will show how one of them, the algebraic coupling of matrix pencils (ACMP) algorithm, can be efficiently applied to our sampling problem. A more detailed discussion of the method can be found in [17].

E. Outline of the ACMP Algorithm

Let the $K(P-L) \times L(Q-K)$ enhanced matrix J be defined as

$$J = \begin{pmatrix} G^{(1,1)} & G^{(2,1)} & \dots & G^{(L,1)} \\ G^{(1,2)} & G^{(2,2)} & \dots & G^{(L,2)} \\ G^{(1,K)} & G^{(2,K)} & \dots & G^{(L,K)} \end{pmatrix} \tag{29}$$

where the (k,l)th block component of J is given by (30), shown at the bottom of the page. The matrix J can be written as

$$J = W' A Z' \tag{31}$$

where W' and Z' are generalized Vandermonde matrices

$$W' = \begin{pmatrix} W_{P-L}^T & Z_d W_{P-L}^T & Z_d^2 W & \dots & Z_d^{K-1} W_{P-L}^T \end{pmatrix} \tag{32}$$

$$Z' = \begin{pmatrix} Z_{Q-K}^T & W_d Z_{Q-K}^T & W_d^2 & \dots & W_d^{L-1} Z_{Q-K}^T \end{pmatrix} \tag{33}$$

W_d and Z_d are $M \times M$ diagonal matrices $W_d = \text{diag}\{e^{i\omega_0 x_k}\}$, $Z_d = \text{diag}\{e^{i\omega_0 y_k}\}$, while W_{P-L} and Z_{Q-K} are given by

$$W_{P-L} = \begin{pmatrix} 1 & 1 & 1 & \dots & 1 \\ w_1 & w_2 & w_3 & \dots & w_M \\ \vdots & & & & \\ w_1^{P-L-1} & w_2^{P-L-1} & w_3^{P-L-1} & \dots & w_M^{P-L-1} \end{pmatrix} \tag{34}$$

$$Z_{Q-K} = \begin{pmatrix} 1 & z_1 & z_1^2 & \dots & z_1^{Q-K-1} \\ 1 & z_2 & z_2^2 & \dots & z_2^{Q-K-1} \\ \vdots & & & & \\ 1 & z_M & z_M^2 & \dots & z_M^{Q-K-1} \end{pmatrix}. \tag{35}$$

Define a top-left matrix J_{tl} obtained by omitting the last row and the last column of the block components of J, i.e. the top-left matrix J_{tl} has block components

$$J_{tl,kl} = \underline{G^{(l,k)}}| = G_{l:P-L-2+l,k:Q-K-2+k} \tag{36}$$

where $(\cdot)|$ denotes the operation of deleting the last column of $(\cdot)$, whereas $\underline{(\cdot)}$ denotes the operation of deleting the last row of $(\cdot)$. Define in a similar way top-right and bottom-left matrices J_{tr} and J_{bl}. The outline of the ACMP algorithm is then the following.

- Compute the singular value decomposition of J_{tl}

$$J_{tl} = USV^H. \tag{37}$$

- Find C_{tr}, C_{tl}, C_{bl}, and C_{br} from

$$U^H(J_{tr} - \mu J_{tl})V = F(Z_d - \mu I)G = C_{tr} - \mu C_{tl} \tag{38}$$

$$U^H(J_{bl} - \mu J_{tl})V = F(W_d - \lambda I)G = C_{bl} - \lambda C_{tl}. \tag{39}$$

- Compute the eigenvalue decomposition of a matrix $C_{tl}^{-1}(\beta C_{tr} + (1-\beta)C_{bl})$

$$C_{tl}^{-1}\left(\beta C_{tr} + (1-\beta)C_{bl}\right) = G^{-1} T G \tag{40}$$

  where β is a scalar introduced with the aim of avoiding multiple eigenvalues.
- Apply the eigentransformation T to $C_{tl}^{-1}C_{tr}$ and $C_{tl}^{-1}C_{bl}$ to find Z_d and W_d, i.e.,

$$T\left(C_{tl}^{-1}C_{bl}\right)T^{-1} = W_d \tag{41}$$

$$T\left(C_{tl}^{-1}C_{tr}\right)T^{-1} = Z_d. \tag{42}$$

Since the same transformation is used to diagonalize both matrices, w_i and z_i correspond to the same sinusoidal component. A necessary condition for this property to hold is that all the matrices involved in the two matrix pencils $J_{tr} - \mu J_{tl}$ and $J_{bl} - \lambda J_{tl}$ can be written as the product of the same left and right matrices,

$$J_{kl} = G^{(l,k)} = \begin{pmatrix} G[l,k] & \dots & G[l, Q-K-1+k] \\ G[l+1,k] & \dots & G[l+1, Q-K-1+k] \\ \vdots & & \\ G[P-L-1+l,k] & \dots & G[P-L-1+l, Q-K-1+k] \end{pmatrix} \tag{30}$$

with possibly a different matrix in the middle. On the other hand, a sufficient condition for Y' and Z' to have the full rank M is

$$P - L \geq M \quad K, L \geq M \quad Q - K \geq M. \tag{43}$$

Equation (43) implies that if we set $L = K = M$, the sufficient condition for having a unique solution is $P \geq 2M$, $Q \geq 2M$. In other words, it suffices to know $G[m, n]$, $m, n \in [-M, M]$;[2] therefore, only $\mathcal{O}(M^2)$ samples of $g(x, y)$ will yield a unique solution for the set of pairs (w_i, z_i). Note that $G[m, n]$ do not necessarily have to correspond to the lowpass version of the signal, and it is possible to obtain a perfect reconstruction from any subspace of the same dimension. While this is true for deterministic signals, in the presence of noise, it is desirable to use oversampled schemes and estimate the signal parameters from a frequency band where a signal-to-noise ratio (SNR) is highest.

Finally, the corresponding set of weights $\{a_i\}$ can be found from (31), i.e., $A = W'^{+} J Z'^{+}$, where $(\cdot)^{+}$ denotes a pseudoinverse of $(\cdot)$. Since both W' and Z' are of rank M, the above system will have a unique solution for the matrix of coefficients A. This leads us to the following proposition.

Proposition 2: Consider a periodic set of M weighted 2-D Diracs $g(x, y)$ having periods $T_x = T_y = T$ in the x and y directions, and let $\varphi(x, y)$ be the 2-D sinc sampling kernel of bandwidth $[-M\omega_0, M\omega_0] \times [-M\omega_0, M\omega_0]$. If the sampling periods T_{sx} and T_{sy} are such that $N_{sx} = T/T_{sx} \geq 2M + 1$ and $N_{sy} = T/T_{sy} \geq 2M + 1$, where $\{N_{sx}, N_{sy}\} \in \mathbb{N}$, then in the general case, the samples

$$y_s[p, q] = \langle g(x, y), \varphi(x - pT_{sx}, y - qT_{sy}) \rangle \quad p \in [0, N_{sx} - 1], \quad q \in [0, N_{sy} - 1]$$

are a sufficient characterization of $g(x, y)$.

In our analysis, we specifically considered the sinc sampling kernel because it allows for a straightforward computation of the Fourier series coefficients of the signal from the set of samples. However, we can use any bandlimited kernel whose spectrum Φ is nonzero over the same region $[-M\omega_0, M\omega_0] \times [-M\omega_0, M\omega_0]$, assuming that the inverse of Φ over that frequency range exists and is numerically stable. That is, the only modification is that the Fourier series coefficients of the sampled signal have to be divided by the corresponding Fourier series coefficients of the sampling kernel before running the estimation algorithm. This allows us to use the same approach based on the shift-invariant subspace property together with a much wider class of antialiasing filters.

F. Point Spread Function

The previous results can be directly extended to the case of signals modeled as a "blurred" version of the set of Diracs or, more precisely, as a convolution of the signal $g(x, y)$ with a certain point spread function (PSF). This case is of interest to the field of optical astronomy, where the image formation, without noise, can be modeled as a convolution of the object being made up of point sources (i.e. stars) with the PSF, which may be a result of the imperfections of imaging optics, atmospheric processes, etc.

[2]In our case $G[m, n]$ are the Fourier series coefficients of $g(x, y)$.

There is no exact expression describing the shape of the PSF; however, many authors [11], [13] prefer to model the blurring process due to the atmospheric turbulence by a Gaussian function of the form

$$h(x, y) \propto \exp\left[-\frac{(x^2 + y^2)}{2\sigma_s^2}\right] \tag{44}$$

or, equivalently, in the frequency domain, as

$$H(\omega_x, \omega_y) \propto \exp\left[-\frac{(\omega_x^2 + \omega_y^2)}{2\sigma_f^2}\right] \tag{45}$$

which turns out to be a good approximation in the case of aberration-free imaging optics. Clearly, the only modification of the sampling scheme is that we have to deconvolve a blurred signal prior to estimating relevant parameters. This can be done in the frequency domain by multiplying the Fourier series coefficients of the blurred signal with the inverse of H. Under the noise-free assumption, this step is sufficient to obtain a set of coefficients that can be expressed as a linear combination of exponentials. However, this step is appropriate if the parameter σ_f is sufficiently large so that finding the inverse of H over the frequency range of interest ($[-M\omega_0, M\omega_0] \times [-M\omega_0, M\omega_0]$) is numerically stable. While the above analysis is valid for periodic signals, the method does not substantially change in the case of finite length signals, which is of more practical importance and will be discussed in the next section.

IV. Finite Length Signals

The previous results on sampling the 2-D point process have been derived under the assumption that the signal is modeled as a periodic pattern of Diracs so that the relevant parameters can be extracted from the appropriate set of the Fourier series coefficients. In this section, we analyze the problem of sampling 2-D signals made up of a finite number of weighted Diracs.

Let a signal $g(x, y)$ be given by

$$g(x, y) = \sum_{i=0}^{M-1} a_i \delta(x - x_i, y - y_i). \tag{46}$$

Consider the samples obtained by filtering the signal with the Gaussian kernel $\varphi_g(x, y) = e^{-(x^2+y^2)/2\sigma^2}$ taken at (mT, nT)

$$g[m, n] = \sum_{i=0}^{M-1} a_i e^{\frac{-\left((x_i - mT)^2 + (y_i - nT)^2\right)}{2\sigma^2}} \tag{47}$$

$$= \sum_{i=0}^{M-1} a_i e^{-\frac{\left(x_i^2 + y_i^2\right)}{2\sigma^2}} e^{\frac{(mx_i + ny_i)}{\sigma^2}} e^{-\frac{(m^2+n^2)T^2}{2\sigma^2}}. \tag{48}$$

Extending a technique used in [20], let us denote $\tilde{g}[m, n] = g[m, n] e^{(m^2+n^2)T^2/2\sigma^2}$ and $c_i = a_i e^{-(x_i^2+y_i^2)/2\sigma^2}$. Then, (48) reduces to

$$\tilde{g}[m, n] = \sum_{i=0}^{M-1} c_i e^{\frac{mx_i}{\sigma^2}} e^{\frac{ny_i}{\sigma^2}}. \tag{49}$$

The set of modified samples $\tilde{g}[m, n]$ can thus be expressed as a linear combination of real exponentials, and in order to deter-

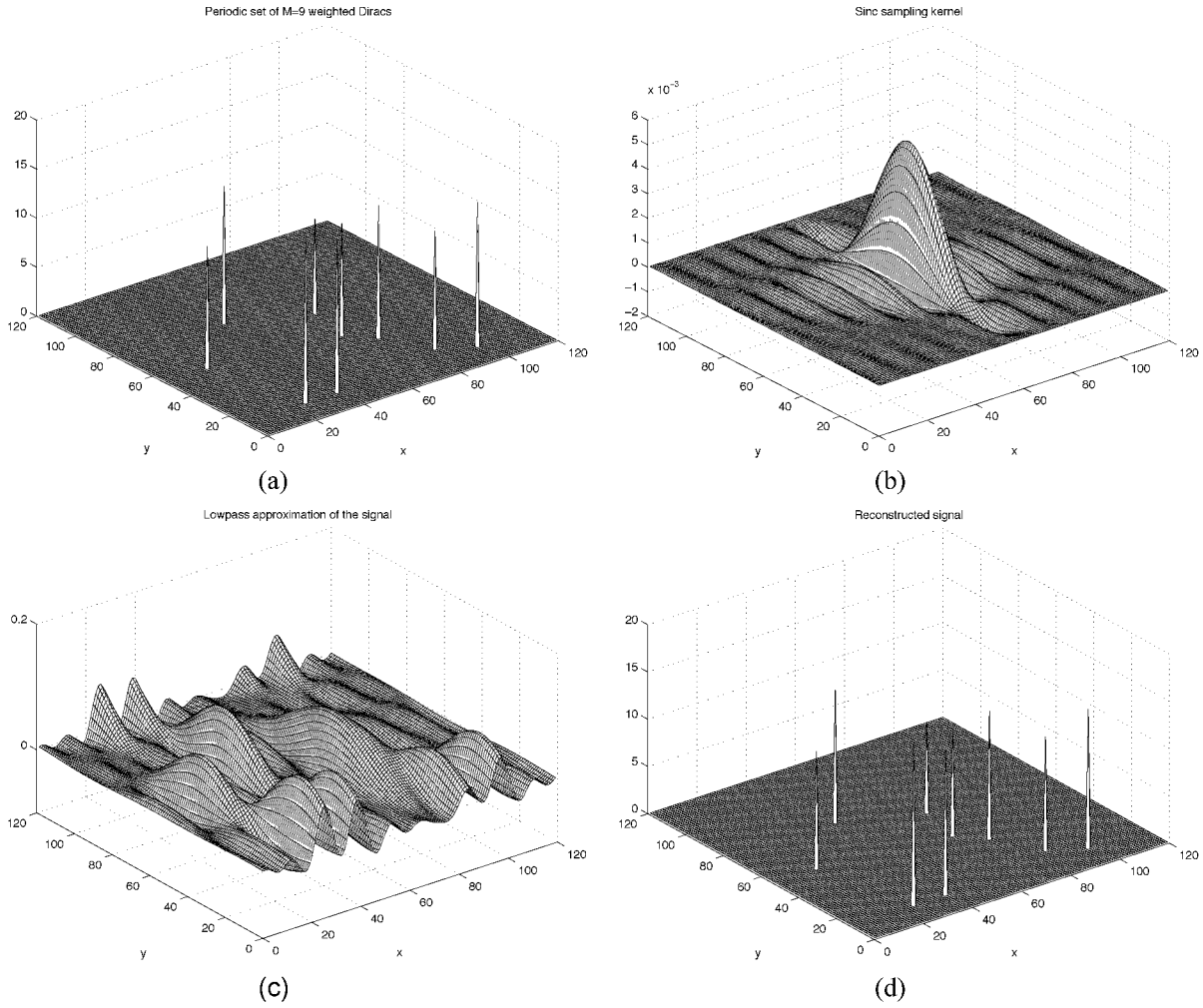

Fig. 2. Annihilating filter method. (a) Two-dimensional signal made up of $M = 9$ weighted Diracs. (b) 2-D sinc sampling kernel of bandwidth $[-M\omega_0, M\omega_0] \times [-\omega_0, \omega_0]$. (c) Lowpass approximation obtained by convolving the signal with the sinc function. (d) Reconstructed signal.

mine a_i and (x_i, y_i), we can apply the method described in the previous section. Thus, we have the following proposition.

Proposition 3: Consider a finite set of M weighted 2-D Diracs $g(x, y)$, and let $\varphi_g(x, y)$ be the Gaussian sampling kernel $\varphi_g(x, y) = e^{-(x^2+y^2)/2\sigma^2}$. If $N_{sx} \geq 2M + 1$ and $N_{sy} \geq 2M + 1$, then the $N_{sx}N_{sy}$ sample values

$$y_s[p, q] = \langle g(x, y), \varphi_g(x - pT, y - qT) \rangle \qquad p \in [0, N_{sx} - 1], \quad q \in [0, N_{sy} - 1]$$

are sufficient to reconstruct the signal.

Note that if the problem is separable in the x or the y direction, the above result holds for the sinc kernel as well, yet the algorithm becomes more complicated [20]. The Gaussian kernel, however, is more important in practical applications. Besides, it allows for an almost local reconstruction, due to the exponential decay of the Gaussian function. In the presence of noise, the width of the reconstruction window must be chosen carefully; otherwise, the system can become ill-conditioned, as we will show in Section VII. While in the separable case there are methods to improve the numerical behavior of the algorithm [4], they cannot be directly extended to the nonseparable problem, and improving the conditioning of the system in such a case is still an open question.

V. Generalization of the Results on 2-D Diracs

The results we derived so far can be applied to a larger class of 2-Dsignals, such as simple lines, polygonal lines, as well as some simple 2-D objects. Although the extensions are not straightforward and typically become more intricate as we increase the complexity of the model, our results still indicate that developing new sampling schemes for such objects is rather intriguing and potentially entails many interesting applications.

A. Line of Finite Length

Consider a periodic signal $g(x, y)$ represented within one period as

$$g(x, y) = \begin{cases} \delta(y - (ax + b)), & x_1 \leq x \leq x_2 \\ 0, & \text{otherwise.} \end{cases} \tag{50}$$

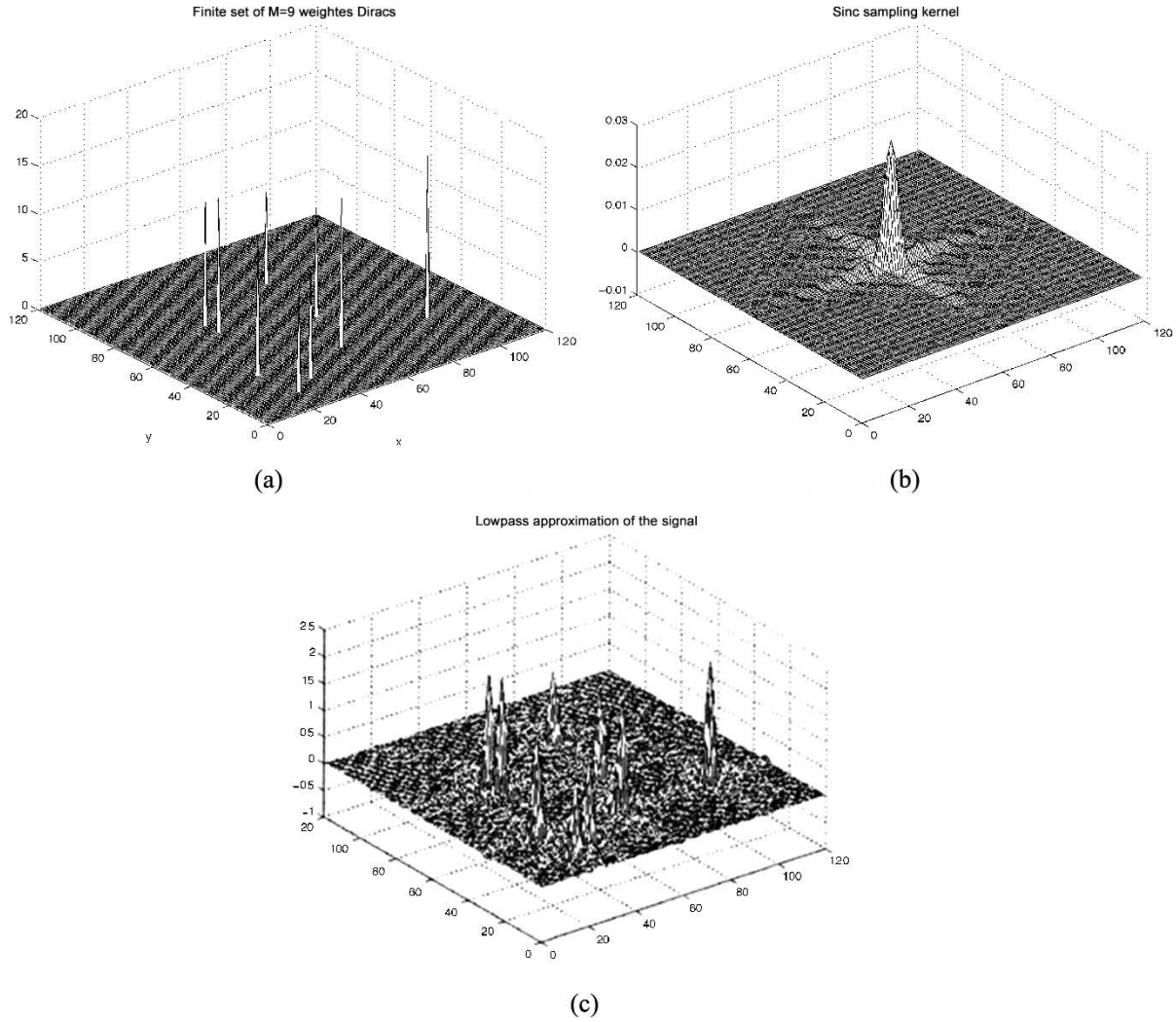

Fig. 3. ACMP algorithm. (a) Signal made up of $M = 9$ weighted Diracs that have common components along both directions. (b) Sinc sampling kernel of bandwidth $[-M\omega_0, M\omega_0] \times [-M\omega_0, M\omega_0]$ used in the algorithm. (c) Lowpass approximation of the signal.

The above notation assumes that the line is not vertical; otherwise, a similar expression can be written by swapping x and y. The Fourier series coefficients of $g(x, y)$ are given by

$$G[m,n] = \frac{1}{T^2}\int_0^T\int_0^T g(x,y)e^{-jm\omega_0 x}e^{-jn\omega_0 y}dxdy \tag{51}$$

$$= \frac{1}{T^2}\int_{x=x_1}^{x=x_2} e^{-jm\omega_0 x} \times \left(\int_0^T \delta\left(y-(ax+b)\right)e^{-jn\omega_0 y}dy\right)dx \tag{52}$$

$$= \frac{1}{T^2}\int_{x=x_1}^{x=x_2} e^{-jm\omega_0 x}e^{-jn\omega_0(ax+b)}dx \tag{53}$$

$$= \frac{e^{-jm\omega_0 x_1}e^{-jn\omega_0 y_1} - e^{-jm\omega_0 x_2}e^{-jn\omega_0 y_2}}{j2\pi T^2(m+na)} \tag{54}$$

Clearly, $G[m, n]$ no longer has the form of a linear combination of complex exponentials since both m and n appear in the denominator. Therefore, neither the annihilating filter method nor the subspace methods can be used directly with the set of the Fourier series coefficients. Yet, the problem can be handled in the following way. Consider the coefficients $G[m, 0]$

$$G[m,0] = \frac{e^{-jm\omega_0 x_1} - e^{-jm\omega_0 x_2}}{j2\pi T^2 m} \tag{55}$$

and define $\widetilde{G}[m] = j2\pi T^2 mG[m, 0] = e^{-jm\omega_0 x_1} - e^{-jm\omega_0 x_2}$. Since $x_1 \neq x_2$,[3] we can solve for the set $\{x_1, x_2\}$ by using the 1-D annihilating filter $H(z)$ with zeros $z_1 = e^{-j\omega_0 x_1}$ and $z_2 = e^{-j\omega_0 x_2}$. The filter coefficients $H[m] = \text{coeff}(H(z))$ can be found from the system of equations $H[m] * \widetilde{G}[m] = 0$, $m \in [-2, 2]$.

Next, consider the coefficients $G[m, 1]$

$$G[m,1] = \frac{e^{-jm\omega_0 x_1}e^{-j\omega_0 y_1} - e^{-jm\omega_0 x_2}e^{-j\omega_0 y_2}}{j2\pi T^2(m+a)}. \tag{56}$$

[3]We assumed that the line is not vertical, otherwise we have to consider the coefficients $G[0, n]$.

There are three unknowns y_1, y_2, and a that can be found from $G[m,1], m \in [-2,2]$. Along with the set $\{x_1, x_2\}$, this uniquely defines the line.

B. Polygonal Line

A straightforward extension of the previous result is the case of a 2-D signal $g(x,y)$ made up of a periodic pattern of a polygonal line, that is, a closed curve made up of a finite number of linear pieces. Let the vertices be located at points (x_i, y_i), $i = 1, 2, \ldots, M$. Since we can think of $g(x,y)$ as being composed of M lines, the Fourier series coefficients $G[m,n]$ can be found using (54)

$$G[m,n] = \frac{e^{-jm\omega_0 x_1} e^{-jn\omega_0 y_1}}{j2\pi T^2} \left[\frac{1}{m+na_1} - \frac{1}{m+na_M}\right] + \frac{e^{-jm\omega_0 x_2} e^{-jn\omega_0 y_2}}{j2\pi T^2} \left[\frac{1}{m+na_2} - \frac{1}{m+na_1}\right] + \ldots + \frac{e^{-jm\omega_0 x_M} e^{-jn\omega_0 y_M}}{j2\pi T^2} \left[\frac{1}{m+na_M} - \frac{1}{m+na_{M-1}}\right].$$

The above relation holds if there are no vertical segments in the signal and is obtained after grouping the terms with the same denominator. Consider the set of coefficients $G[0,n], n \in [-M, M]$:

$$G[0,n] = \frac{e^{-jn\omega_0 y_1}}{j2\pi T^2} \left[\frac{1}{na_1} - \frac{1}{na_M}\right] + \frac{e^{-jn\omega_0 y_2}}{j2\pi T^2} \times \left[\frac{1}{na_2} - \frac{1}{na_1}\right] + \ldots + \frac{e^{-jn\omega_0 y_M}}{j2\pi T^2} \left[\frac{1}{na_M} - \frac{1}{na_{M-1}}\right]$$

and let $\widetilde{G}[n] = j2\pi T^2 n G[0,n]$

$$\widetilde{G}[n] = \sum_{k=1}^{N} c_k e^{-j\omega_0 n y_k} \quad n \in \mathbb{Z} \tag{57}$$

where $c_k = 1/a_k - 1/a_{k-1}$. Since $\widetilde{G}[n]$ has the form of a weighted sum of complex exponentials, the sets $\{y_i\}$ and $\{c_i\}$ can be found from the coefficients $\widetilde{G}[n]$, $n \in [-M, M]$ using the annihilating filter method. In order to obtain a unique solution, two conditions need to be satisfied. Namely, all y_i must be different, and none of the coefficients c_i should be equal to zero. The second condition is always satisfied, given the fact that the adjacent segments of the polygonal line must have different slopes (a_{k-1} and a_k). On the other hand, the first condition poses further constraints on the location of the vertices.

Next, consider a set of coefficients $G[1,n]$ $n \in [-M, M]$ given by

$$G[1,n] = \frac{e^{-j\omega_0 x_1} e^{-jn\omega_0 y_1}}{j2\pi T^2} \left[\frac{1}{1+na_1} - \frac{1}{1+na_M}\right] + \ldots + \frac{e^{-j\omega_0 x_M} e^{-jn\omega_0 y_M}}{j2\pi T^2} \left[\frac{1}{1+na_M} - \frac{1}{1+na_{N-1}}\right]. \tag{58}$$

The above relation is a system of $2M$ nonlinear equations with $2M$ unknowns that can be solved for $z_i = e^{-j\omega_0 x_i}$ and a_i. Together with the corresponding values y_i, this uniquely defines the polygonal line.

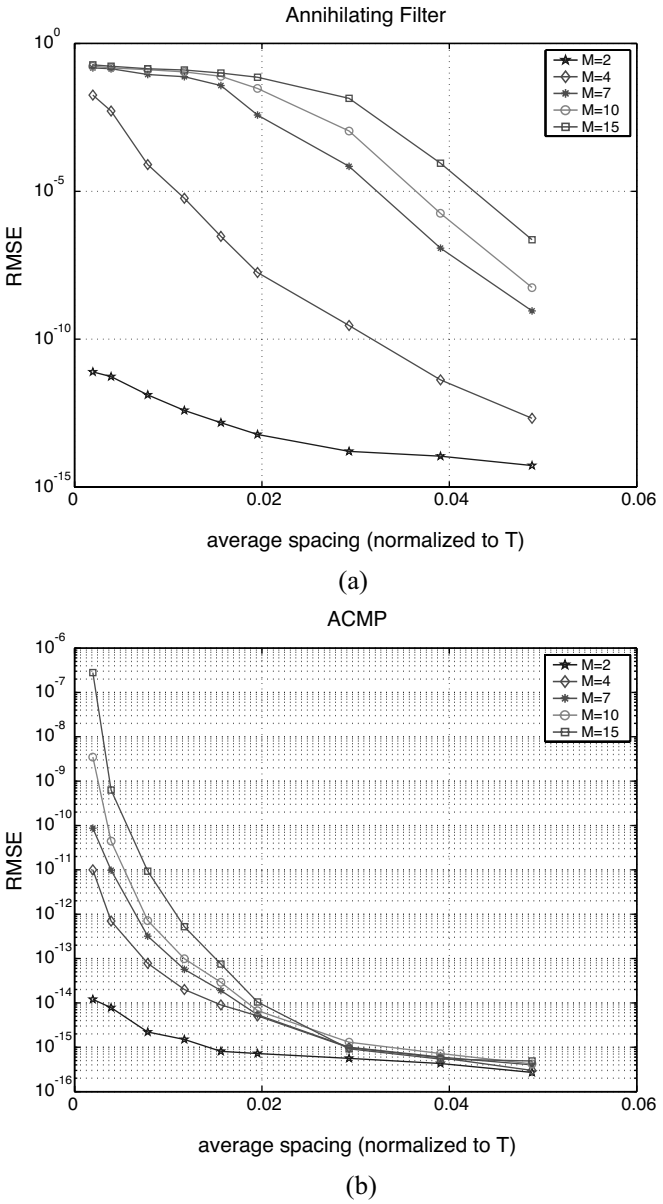

Fig. 4. Numerical performance versus average spacing of the Diracs. The numerical behavior of the algorithms is tested for different values of the average spacing (normalized to one period) of M Diracs in the set, as well as for different values of M. (a) Average reconstruction error for the annihilating filter algorithm. (b) Average reconstruction error for the ACMP algorithm.

While all the signal parameters can be extracted from the above set of samples, the described method includes solving the system of nonlinear (58), which may yield a mediocre numerical precision and high complexity. One possible way to overcome this problem is to solve separately for the x and the y coordinates of vertices and then use a combinatorial approach, that is, find a set of pairs (x_i, y_i) that best matches the lowpass approximation obtained from the samples. Although this solution requires twice the number of samples compared with the previous method and involves an optimization procedure as well, its numerical precision is typically much better. Clearly, both methods yield a solution by taking $\mathcal{O}(M)$ samples; however, the necessary condition for their success is that the vertices of the polygonal line have no common components along the x and y directions.

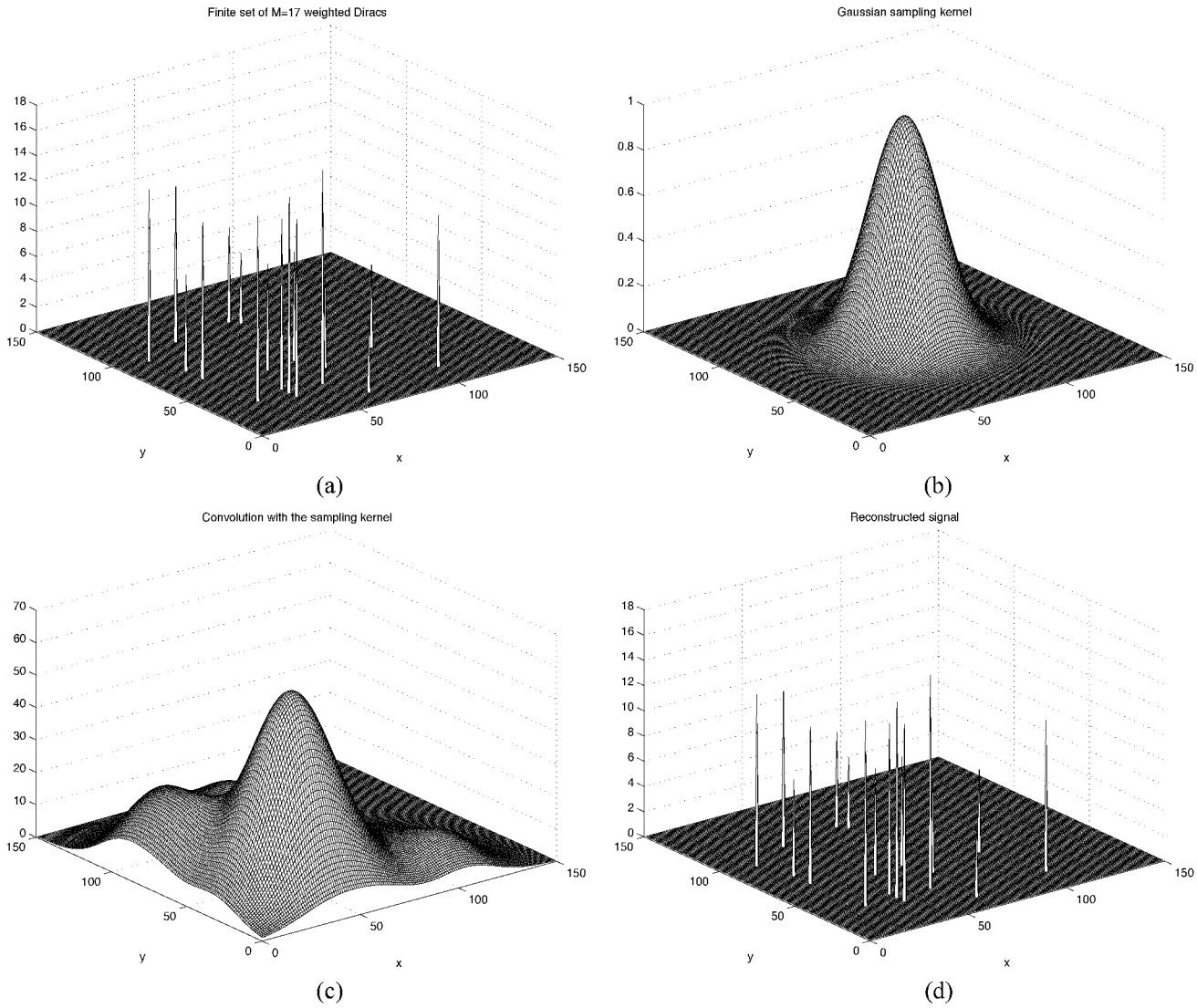

Fig. 5. Finite set of 2-D Diracs. (a) Two-dimensional signal made up of $M = 17$ weighted Diracs. (b) Gaussian sampling kernel. (c) Convolution of the signal with the sampling kernel. (d) Reconstructed signal with an RMSE of less than 10^{-8}.

C. Bilevel 2-D Signals

A further extension of the previous results includes the case of a bilevel signal $g(x, y)$ made up of a periodic pattern of polygons. As in the previous case, assume that $g(x, y)$ does not contain vertical lines. Under this assumption, we can take a partial derivative with respect to y, and by denoting $g_y(x, y) = ((\partial g(x, y))/\partial y)$, we get

$$\frac{\partial g(x,y)}{\partial y} = \sum_{m=-\infty}^{\infty} \sum_{n=-\infty}^{\infty} G[m,n] jn\omega_0 e^{jm\omega_{0x}x} e^{jn\omega_{0y}y} = \sum_{m=-\infty}^{\infty} \sum_{n=-\infty}^{\infty} G_y[m,n] e^{jm\omega_0 x} e^{jn\omega_0 y}. \quad (59)$$

Since $g_y(x, y)$ is a signal made up of a polygonal line, its Fourier series coefficients are given by

$$G_y[m,n] = j\omega_0 n G[m,n]. \quad (60)$$

Therefore, instead of taking a derivative of the signal itself, the derivation can be done on the Fourier series coefficients, and the values $G_y[m, n]$ should be used in the algorithm developed in Section III.

VI. Numerical Performance and Algorithms in the Presence of Noise

So far, we have assumed deterministic signals and considered the possibility of developing the sampling schemes that allow for perfect reconstruction from as few samples as possible. Questions that naturally arise from this approach are related to numerical precision and stability of the developed algorithms as well as to their performance in the presence of noise.

A. Complexity

In Section II, we proved that under certain conditions, the annihilating filter algorithm leads to perfect reconstruction from only $\mathcal{O}(M)$ samples. However, in the presence of noise, this approach has several disadvantages. Namely, the annihilating filter method is basically a 1-D approach, that is, the coordinates of Diracs along one direction are estimated

by finding the roots of the annihilating filter, whereas the corresponding coordinates along the other direction are then found by solving a Vandermonde system (i.e., the information is extracted from a set of weighting coefficients). In general, the root-finding part of the algorithm is more robust to noise than the estimation of the weighting coefficients, which then results in a different numerical precision in the x and y directions. Besides, even in the case of noiseless data, the numerical accuracy of the method decreases if there are closely spaced Diracs in the set (particularly for large values of M), due to the root-finding part of the algorithm. On the other hand, the approach based on 2-D subspace methods exploits the shift-invariance property and relies only on a right deployment of matrix manipulations. It avoids the problem of different precision in x and y and typically yields better performances at the expense of a higher computational complexity. The major computational requirement of the annihilating filter method is associated with the root-finding part of the algorithm so that the overall computational order is $\mathcal{O}(M^2 \log M)$. On the other hand, the computational requirement of the ACMP algorithm is dominated by the SVD of the $M^2 \times M^2$ matrix J_{tl}, which results in the overall order of $\mathcal{O}(M^6)$.

B. Noisy Case

In the case of noisy signals, critically sampled schemes typically result in poor numerical accuracy. In practice, this problem can be dealt with by using oversampling and truncation of the SVD of certain matrices. For example, we can exploit this idea to modify the ACMP algorithm presented in Section III. Since the presence of noise destroys the low rank property of the matrix J_{tl} defined in (36), we have to truncate the SVD of J_{tl} explicitly to rank M, i.e.,

$$J_{tl} = USV^H + U_n S_n V_n^H \tag{61}$$

with S being a full-rank $M \times M$ matrix. The presence of noise thus necessarily degrades the performance of the algorithm due to the fact that the eigentransformation T will no longer perfectly diagonalize both matrix pencils.

The same approach can be used to modify the annihilating filter method, that is, we should consider an extended system of (21)

$$\sum_{i=1}^{M} h_i G[m-i,1] = -G[m,1],\ m = 1,2,\ldots,M_1,\ M_1 > M \tag{62}$$

and decompose a matrix of coefficients $\mathbf{G}$ as

$$\mathbf{G} = \begin{pmatrix} G[0,1] & G[-1,1] & \cdots & G[1-M,1] \\ G[1,1] & G[0,1] & \cdots & G[2-M,1] \\ \vdots & \vdots & \ddots & \\ G[M_1-1,1] & G[M_1-2,1] & \cdots & G[M_1-M,1] \end{pmatrix} = U_g \Lambda_g V_g^H + U_n \Lambda_n V_n^H \tag{63}$$

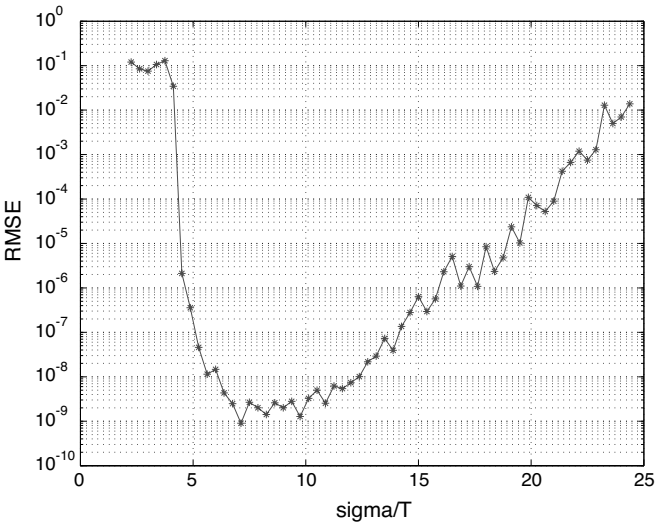

Fig. 6. Numerical precision versus width of the Gaussian kernel. The signal from Fig. 4(a) is sampled with the Gaussian kernel $e^{-((x^2+y^2)/2\sigma^2)}$. The parameter σ is varied between $0.03T$ and $25T$, where T denotes the spacing between adjacent samples. The reconstruction error is plotted as a function of σ/T, indicating a strong sensitivity to the choice of the width σ.

where the first term corresponds to the best (in the Frobenius-norm sense) rank M approximation of the matrix $\mathbf{G}$. The filter coefficients H are then computed as

$$H = -V_g \Lambda_g^{-1} U_g^H \cdot \begin{pmatrix} G[1,1] \\ G[2,1] \\ \vdots \\ G[M_1,1] \end{pmatrix}. \tag{64}$$

C. Estimation of the Model Order and Model Mismatch

Note that in the methods presented so far, we required prior knowledge of the model order M. Therefore, an obvious question is how do we know in advance the number of parameters that have to be estimated? This question is at the core of a model-based approach to nonlinear estimation problems encountered in signal and data analysis [5], [12]. For example, if we use the ACMP algorithm, M can be estimated as the number of dominant singular values of J_{tl}, which is a very good estimate of the model order if the smallest singular value of the original low-rank matrix J_{tl} is not dominated by the noise variance. On the other hand, for low values of SNR, it is often difficult to discriminate between small singular values corresponding to the signal from extraneous ones due to noise, and typically, only dominant signal components can be reliably estimated. That is, in such a case, overmodeling the signal can give rise to spurious poles that can be incorrectly identified as signal poles. Similarly, if the annihilating filter algorithm is used, the number of dominant singular vectors of the extended matrix $\mathbf{G}$ (assuming that the number of columns is greater than M) should be used as an estimate of the model order. A more detailed treatment of this problem can be found in [5].

Another interesting question is how well we can reconstruct the signal if the number of samples is less than the minimum number theoretically required for perfect reconstruction? Intuitively, if the signal has only $K < M$ dominant components,

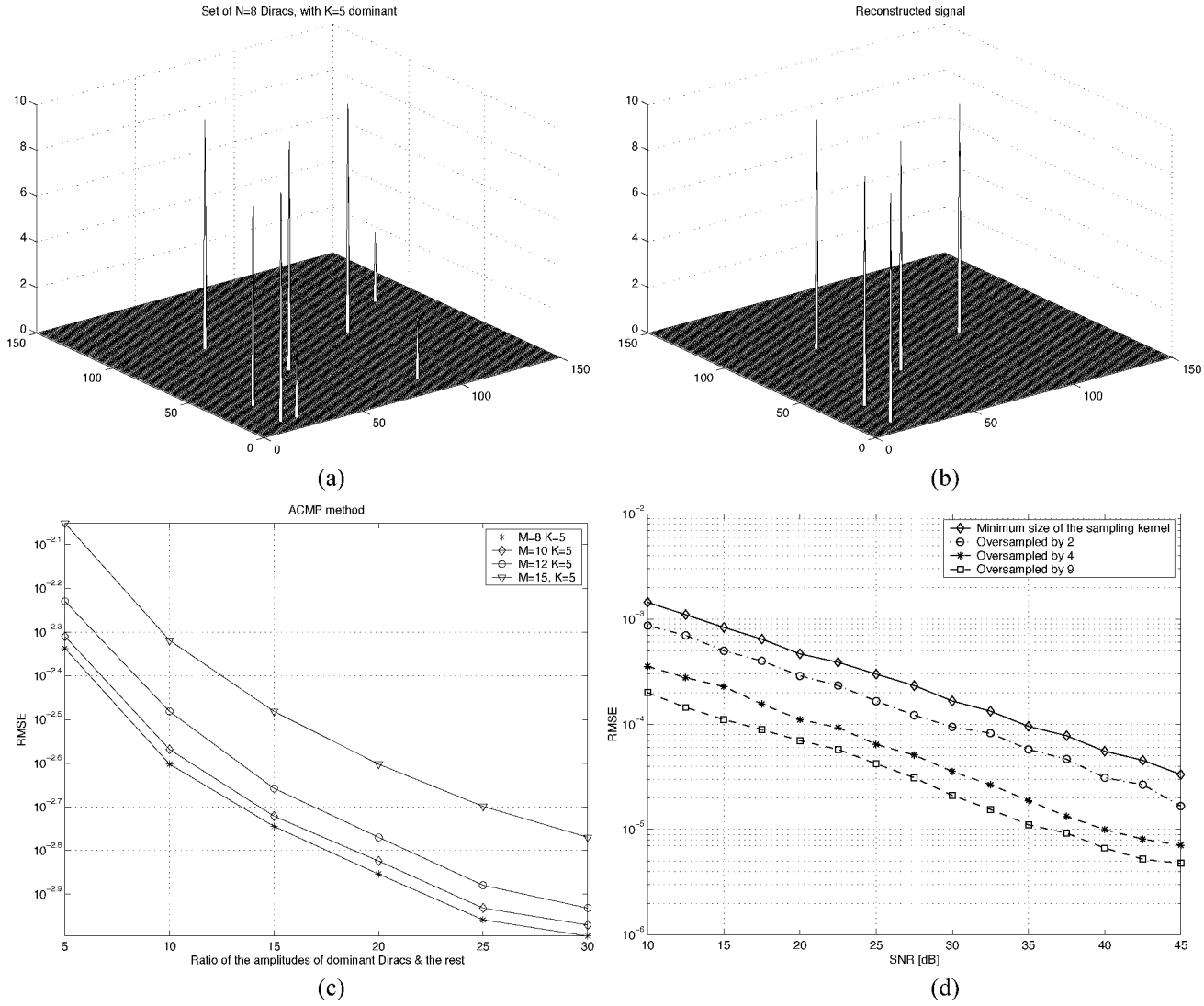

Fig. 7. Model mismatch and performance in the presence of noise. (a) Set of $M = 8$ weighted Diracs with $K = 5$ Diracs being dominant, all having the same weights $a_n = 10$, whereas the rest have weights $a_n = 3$. (b) Reconstructed signal. We assumed that the model order is $M = 5$ and used the ACMP algorithm to reconstruct the signal. Only the dominant components are extracted, with the reconstruction error of RMSE $= 0.006$. (c) Average reconstruction error for different values of the ratio of amplitudes $A_{\text{dominant}}/A_{\text{nondominant}}$ as well as for different number of nondominant components in the set for the ACMP method. (d) Performance of the ACMP algorithm in the noisy case: RMSE versus SNR for different values of the oversampling factor.

one might expect to extract only these components from the undersampled signal, provided that the number of samples is still sufficient for that. This turns out to be true, as we will demonstrate in the next section, which points to some robustness of the algorithms to model mismatch.

VII. Experimental Results

We illustrate the performance of the proposed sampling schemes with some simulation examples. A noiseless periodic signal made up of $M = 9$ weighted Diracs that have common components along the y direction but not along the x direction is presented in Fig. 2(a). The signal is filtered with the sinc sampling kernel of bandwidth $[-M\omega_0, M\omega_0] \times [-\omega_0, \omega_0]$, which is shown in Fig. 2(b), leading to the lowpass approximation in Fig. 2(c). All the signal parameters are estimated using the annihilating filter method, and the reconstructed signal is illustrated in Fig. 2(d). The algorithm provides almost perfect reconstruction in this case, with an RMSE of less than 10^{-12}.

Fig. 3(a) illustrates a noiseless signal consisting of $M = 9$ weighted Diracs that have common components in both directions. Since the annihilating filter method would fail in this case, we will use the ACMP algorithm to recover the signal from its lowpass approximation. The signal is sampled with the sinc sampling kernel, shown in Fig. 3(b), and reconstructed with an RMSE of less than 10^{-13}. However, as opposed to the annihilating filter method, the numerical precision of this algorithm is not considerably affected by the spacing of Diracs in the set. This is shown in Fig. 4, where a reconstruction error is plotted as a function of average spacing D of the Diracs in the set. Clearly, for small values of D, the performance of the annihilating filter method degrades as the number of Diracs increases, whereas the ACMP method retains good numerical properties, even for large values of M.

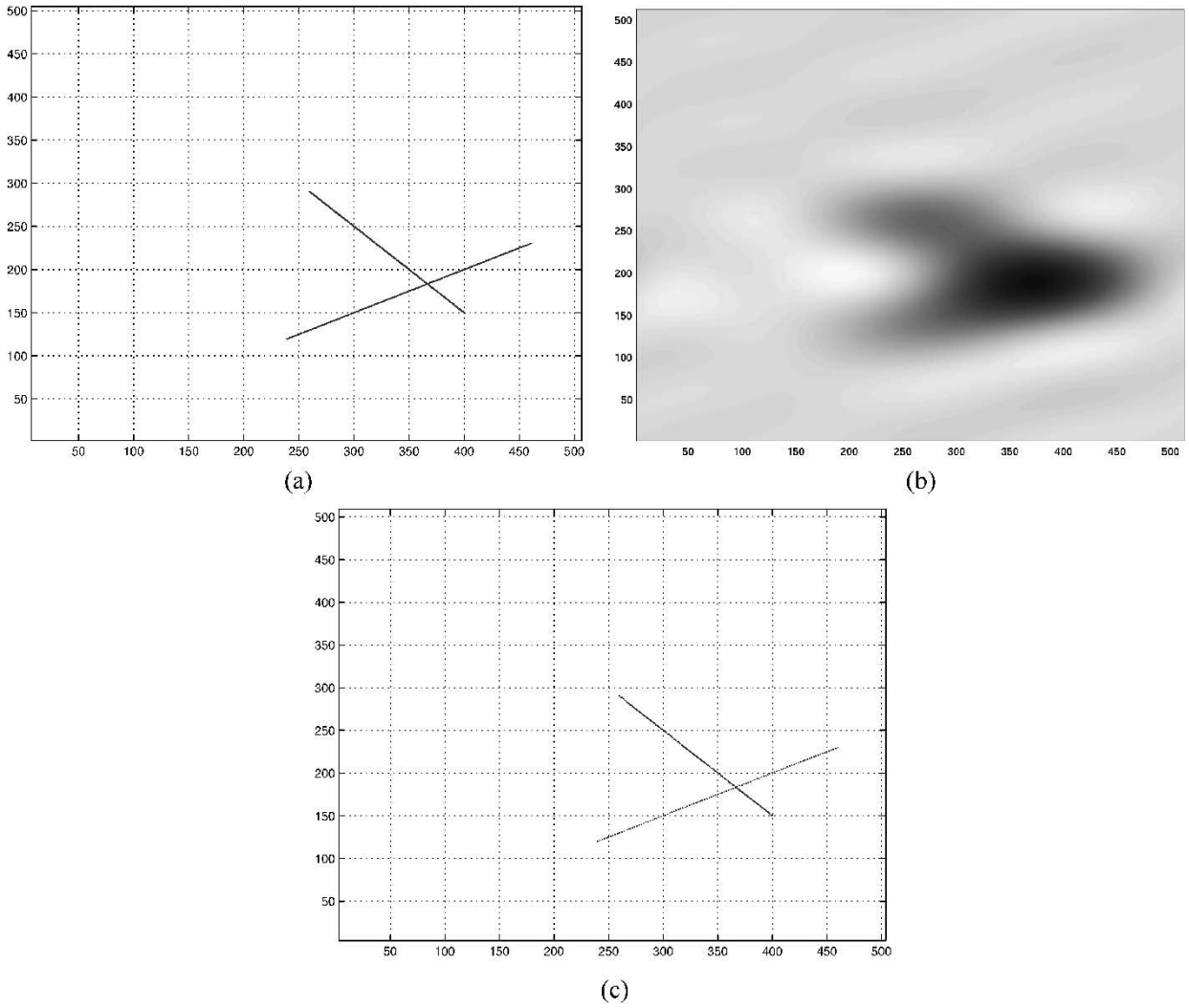

Fig. 8. Set of finite lines. (a) Signal made up of two finite lines. (b) Lowpass approximation obtained by convolving the signal with the sinc kernel of bandwidth $[-4\omega_0, 4\omega_0] \times [-\omega_0, \omega_0]$. (c) Reconstructed set of lines.

The case of finite-length signals, namely finite sets of Diracs, is considered next. Fig. 5(a) illustrates a signal made up of $M = 17$ weighted Diracs. The signal is filtered with the Gaussian kernel shown in Fig. 5(b), and a set of uniform samples is taken from a filtered version shown in Fig. 5(c). The reconstructed signal is presented in Fig. 5(d), and the reconstruction error is less than 10^{-8}. Note that in this case, the width of the Gaussian kernel (i.e. the value of the parameter σ) must be chosen carefully in order to ensure the good numerical performance of the method, as illustrated in Fig. 6.

We next analyze robustness of the algorithms to model mismatch, in particular, how well they perform if the signal is undersampled. Fig. 7(a) shows a signal made up of $M = 8$ weighted Diracs with $K = 5$ of them being dominant. The locations of the Diracs are randomly chosen according to a uniform distribution over [1,150] $\times$ [1,150]. The signal is sampled with the sinc kernel of bandwidth $[-K\omega_0, K\omega_0] \times [-K\omega_0, K\omega_0]$, and the ACMP method is used to find the signal parameters from its lowpass approximation. In Fig. 7(b), we show a reconstructed signal where only the dominant components have been extracted, whereas the precision with which we can estimate them depends on the number of nondominant components and their overall power, as illustrated in Fig. 7(c). Fig. 7(d) shows the behavior of the ACMP algorithm in the presence of noise. We considered the signal made up of eight Diracs, this time having equal weights, embedded in additive white Gaussian noise. The method was tested for different values of a SNR and different values of the sampling kernel bandwidth B_s. For each value of the SNR, as well as B_s, we plotted an average RMSE over 50 different realizations of the signal. The results clearly indicate that the numerical precision of the method is improved by increasing the bandwidth of the sampling kernel and estimating the signal parameters from a larger set of samples. Roughly speaking, in order to reduce the RMSE by a factor of K_s, the bandwidth of the sampling kernel has to be increased K_s times.

Some extensions of the developed sampling schemes to simple objects are considered next. One example is presented in Fig. 8, which demonstrates the performance of the algorithm when applied to a set of two finite lines. The signal is filtered with the sinc kernel of bandwidth $[-4\omega_0, 4\omega_0] \times [-\omega_0, \omega_0]$, leading to a lowpass approximation shown in Fig. 8(b). A set of lines is almost perfectly reconstructed by using the annihilating filter method [see Fig. 8(c)]. Another example is illustrated in Fig. 9(a), that is, sampling a bilevel pentagon.

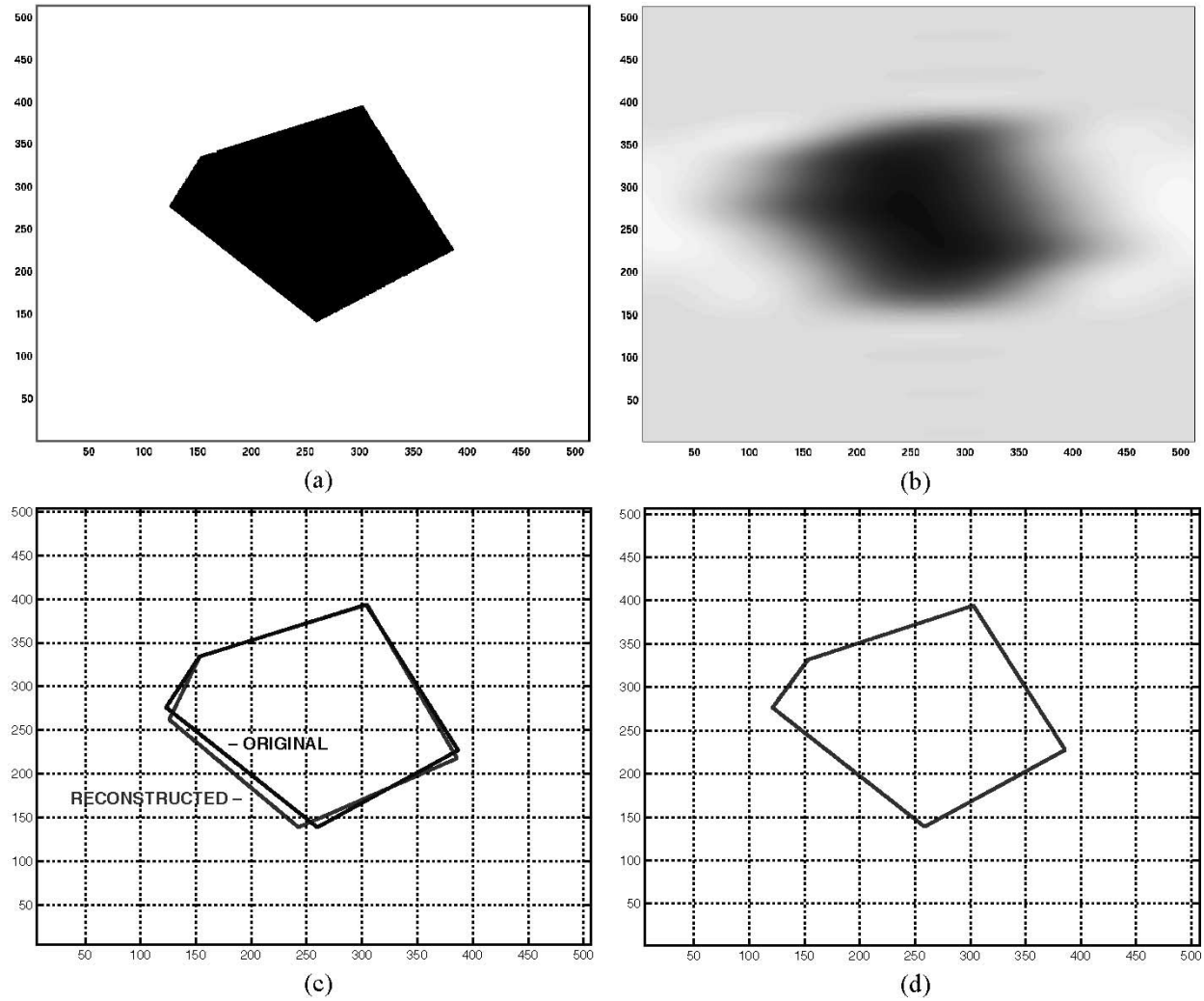

Fig. 9. Bilevel polygon. (a) Bilevel pentagon. The signal has $2M = 10$ degrees of freedom. (b) Lowpass approximation obtained by convolving the signal with the sinc kernel of bandwidth $[-2M\omega_0, 2M\omega_0] \times [-\omega_0, \omega_0]$. (c) Polygonal line reconstructed with the annihilating filter method and the original polygonal line. (d) Polygonal line reconstructed with the state space method. In this case, the line is reconstructed with an RMSE of less than 10^{-4}.

The signal is first filtered with a sinc kernel of bandwidth $[-2M\omega_0, 2M\omega_0] \times [-\omega_0, \omega_0]$ (where $M = 5$), and a set of samples is taken from a lowpass approximation shown in Fig. 9(b). Although the signal is completely specified by this set of samples, we extracted only the x coordinates of vertices from the given set, whereas the y coordinates are found from sample values taken with the sinc kernel of bandwidth $[-\omega_0, \omega_0] \times [-2M\omega_0, 2M\omega_0]$. The reason for doing this is to avoid solving the system of nonlinear equation (58), which typically results in less numerical precision than the above approach. The corresponding pairs (x_i, y_i) are then found by using a combinatorial method, that is, by choosing a set that corresponds to a signal with a lowpass version that best matches the lowpass approximation from Fig. 9(b). Fig. 9(c) shows the polygonal line reconstructed using the annihilating filter method, whereas in Fig. 9(d), a 1-D subspace method (the state space method [12]) is applied, which clearly performs better.

VIII. Conclusion

We have presented several algorithms for sampling certain classes of 2-D signals that are not bandlimited but have a finite number of degrees of freedom. Our approach differs form standard multidimensional sampling schemes since we tried to develop methods that can perfectly reconstruct such signals from a finite set of samples. We analyzed in detail the signal made up of 2-D Diracs, whose algebraic structure gives a good insight into the basic principles inherent in all our algorithms, and discussed possible extensions of the results to more complex classes of signals. In order to derive exact sampling formulas, we used some techniques already encountered in the context of spectral estimation. Although the sampling results were derived under the noise-free assumption, the case of noisy data was considered as well. With the exception of one case that is very sensitive to noise (the nonseparable Gaussian case with finite length signals), the methods have desirable numerical properties, given good choices of parameters and sufficient oversampling. The proposed algorithms potentially have impact in certain signal processing applications like image processing. We are currently looking into one application to super-resolution videogrammetry, where the position of 3-D objects can be determined with subpixel precision by locating some clearly marked features, such as points or edges, using a set of 2-D images taken

from various angles [4]. Finally, we would like to mention that while the methods we presented are rather specific, we believe there is a much larger class of nonbandlimited signals that can be perfectly reconstructed from a finite set of samples. We are investigating some alternative techniques, such as Radon transform sampling, that would be applicable to more general classes of signals, and the first results are promising [9].

ACKNOWLEDGMENT

The authors would like to thank reviewers for their constructive remarks.

REFERENCES

[1] A. Adroubi and K. Grochenig, "Non-uniform sampling in shift-invariant spaces," *SIAM Rev.*, vol. 43, pp. 585–620, 2001.
[2] E. R. Berlekamp, *Algebraic Coding Theory*. New York: McGraw-Hill, 1968.
[3] R. E. Blahut, *Theory and Practice of Error Control Codes*. Reading, MA: Addison-Wesley, 1983.
[4] A. Chebira, P. L. Dragotti, L. Sbaiz, and M. Vetterli, "Sampling and interpolation of the plenoptic function," in *Proc. ICIP*, 2003.
[5] J. J. Fuchs, "Estimating the number of sinusoids in aditive white noise," *IEEE Trans. Acoust. Speech, Signal Processing*, vol. 36, pp. 1846–1853, Dec. 1998.
[6] M. Haardt, M. D. Zoltowski, C. P. Mathews, and J. A. Nossek, "Two-dimensional unitary esprit for efficient 2D parameter estimation," in *Proc. IEEE Int. Conf. Acoust., Speech, Signal Processing*, vol. 3, 1995, pp. 2096–2099.
[7] Y. Hua, "Estimating two-dimensional frequencies by matrix enhancement and matrix pencil," *IEEE Trans. Signal Processing*, vol. 40, pp. 2267–2280, Sept. 1992.
[8] R. Roy and T. Kailath, "ESPRIT estimation of signal parameters via rotational invariance techniques," *IEEE Trans. Acoust., Speech Signal Processing*, vol. 37, pp. 984–995, July 1989.
[9] I. Maravić and M. Vetterli, "A sampling theorem for the Radon transform of finite complexity objects," in *Proc. IEEE Int. Conf. Acoust., Speech, Signal Processing*, vol. 2, May 2002, pp. 1197–1200.
[10] J. L. Massey, "Shift register synthesis and BCH decoding," *IEEE Trans. Inform. Theory*, vol. IT-15, pp. 122–127, Jan. 1969.
[11] R. Molina, J. Nunez, F. J. Cortio, and J. Mateos, "Image restoration in astronomy," *IEEE Signal Processing Mag.*, vol. 18, pp. 11–29, Mar. 2001.
[12] B. D.Bahaskar D. Rao and K. S. Arun, "Model based processing of signals: a state space approach," *Proc. IEEE*, vol. 80, pp. 283–309, Feb. 1992.
[13] R. Molina and B. D. Ripley, "Using spatial models as priors in astronomical image analysis," *J. Appl. Statist.*, vol. 16, pp. 193–206, 1989.
[14] S. Rouquette and M. Najim, "Estimation of frequencies and damping factors by two-dimensional ESPRIT type methods," *IEEE Trans. Signal Processing*, vol. 49, pp. 237–245, Jan. 2001.
[15] P. Stoica and R. Moses, *Introduction to Spectral Analysis*. New York: Prentice-Hall, 2000.
[16] M. Unser, "Sampling-50 years after Shannon," *Proc. IEEE*, vol. 88, pp. 569–587, Apr. 2000.
[17] F. Vanpoucke, M. Moonen, and Y. Berthoumieu, "An efficient subspace algorithm for 2-D harmonic retrieval," in *Proc. IEEE Int. Conf. Acoust., Speech, Signal Processing*, vol. 4, 1994, pp. 461–464.
[18] A. J. Vanderveen, P. Ober, and E. Deprettere, "Azimuth and elevation computation in high resolution DOA estimation," *IEEE Trans. Signal Processing*, vol. 40, pp. 1828–1832, July 1992.
[19] A. J. Vanderveen, M. C. Vanderveen, and A. Paulraj, "Joint angle and delay estimation using shift-invariance techniques," *IEEE Trans. Signal Processing*, vol. 46, pp. 405–418, Feb. 1998.
[20] M. Vetterli, P. Marziliano, and T. Blu, "Sampling signals with finite rate of innovation," *IEEE Trans. Signal Processing*, vol. 50, pp. 1417–1428, June 2002.
[21] ——, "A sampling theorem for periodic piecewise polynomial signals," in *Proc. IEEE Int. Conf. Acoust., Speech, Signal Processing*, May 2001.

Irena Maravić received the B.S. degree from the Department of Electrical Engineering, University of Belgrade, Belgrade, Yugoslavia, in 1997 and the M.S. degree from the California Institute of Technology, Pasadena, in 2000. She is currently pursuing the Ph.D. degree in the filed of digital signal processing at the Swiss Federal Institute of Technology (EPFL), Lausanne, Switzerland.

From 1997 to 1999, she was a member of academic staff at the University of Belgrade. In 2000, she joined the Laboratory for Audio-Visual Communications, EPFL. Her research interests include signal processing for communications, sampling theory, multidimensional signal processing, and computational harmonic analysis.

Martin Vetterli (F'95) received the Dipl. El.-Ing. degree from ETH Zürich (ETHZ), Zürich, Switzerland, in 1981, the M.S. degree from Stanford University, Stanford, CA, in 1982 and the Doctorat ès Science degree the Swiss Federal Institute of Technology (EPFL), Lausanne, Switzerland, in 1986.

He was a Research Assistant at Stanford and EPFL and has worked for Siemens and AT&T Bell Laboratories. In 1986, he joined Columbia University, New York, NY, where he was an Associate Professor of electrical engineering and co-director of the Image and Advanced Television Laboratory. In 1993, he joined the University of California, Berkeley, where he was a Professor with the Department of Electrical Engineering and Computer Sciences until 1997 and now holds an Adjunct Professor position. Since 1995, he has been a Professor of communication systems at EPFL, where he chaired the Communications Systems Division from 1996 to 1997 and was head of the Audio-Visual Communications Laboratory. He held visiting positions at ETHZ in 1990 and Stanford in 1998. He is also on the editorial boards of *Annals of Telecommunications*, *Applied and Computational Harmonic Analysis*, and *The Journal of Fourier Analysis and Applications*. His research interests include wavelets, signal processing for communications, computational complexity, image/video processing and compression, and distributed signal processing and communications. He is the co-author, with J. Kovacevic, of the book *Wavelets and Subband Coding* (Englewood Cliffs, NJ: Prentice-Hall, 1995). He has published about 90 journal papers on a variety of topics in signal/image processing and communications and holds seven patents.

Dr. Vetterli is a member of SIAM and was the Area Editor for Speech, Image, Video, and Signal Processing of the IEEE TRANSACTIONS ON COMMUNICATIONS. He received the Best Paper Award of EURASIP in 1984 for his paper on multidimensional subband coding, the Research Prize of the Brown Bovery Corporation (Switzerland) in 1986 for his doctoral thesis, and the IEEE Signal Processing Society's Senior Award in 1991 and in 1996 (for papers with D. LeGall and K. Ramchandran, respectively). He received the Swiss National Latsis Prize in 1996, the SPIE Presidential award in 1999, and the IEEE Signal Processing Technical Achievement Award in 2001. He is a member of the Swiss Council on Science and Technology. Since 2001, he has directed the National Competence Center in Research on mobile information and communication systems (www.terminodes.org). He was a plenary speaker at various conferences (e.g., 1992 IEEE ICASSP).